Available online at www.CivileJournal.org

Civil Engineering Journal

(E-ISSN: 2476-3055; ISSN: 2676-6957)

Vol. 9, No. 10, October, 2023

Shear Performance of Reinforced Concrete T Beams Strengthened by Carbon Fiber-Reinforced Polymer Bars

Hussain Hassan Alhilli [1*], Mahdi H. Al-Farttoosi [1]

[1] *Department of Civil Engineering, Faculty of Engineering, University of Baghdad, 10071 Baghdad, Iraq.*

Received 15 June 2023; Revised 22 August 2023; Accepted 09 September 2023; Published 01 October 2023

Abstract

The primary purpose of this work is to investigate the shear response of T-reinforced concrete beams strengthened for shear using the embedded through section (ETS) technique when subjected to a monotonic one-point load till failure. The experimental approach included an examination of the twelve reinforced concrete T-beams, including two reference beams without any strengthening and ten strengthened beams. The twelve beams were divided into two main groups, with and without stirrups. The main variables in every group were the spacing and angle of inclination of the carbon fibre-reinforced polymer (CFRP) bars. The beams were strengthened in shear with CFRP bars inserted in the centre line of the section with different spacings and angles of inclination. The experimental analysis was performed to study the effect of spacing and angle of inclination of the CFRP bars on the ultimate load capacity, load-strain relationships, and load-deflection relationships. Results showed that the ultimate load of the beams in group one with inclined CFRP bars (45°) increased by 29.7, 22.4, and 15.5% for beams with CFRP bar spacings of 10, 15, and 20 cm, respectively, compared with the reference beam. In group one (with stirrups), the beam with inclined CFRP bars (45°) and a spacing of 10 cm has an ultimate load higher than that with vertical CFRP bars (90°) with a similar spacing by 2.6%. By contrast, the beam with inclined CFRP bars (45°) and a spacing of 10 cm in group two (without stirrups) has an ultimate load higher than that with vertical CFRP bars (90°) with a similar spacing by 2.5%.

Keywords: T-Beams; CFRP Bars; Embedded Through Section (ETS); Shear Strength.

1. Introduction

During the last three decades of the previous century, the utilisation of carbon fibre-reinforced polymer (CFRP) composites for strengthening reinforced concrete (RC) structures has emerged as a highly promising technology to address the rehabilitation of infrastructure. CFRP strengthening can be used in various ways, including to build new buildings and fix old ones [1–3]. In addition to analysing the general failure criterion of CFRP-RC beams, other researchers have focused on the local behaviour at the bond interface. Several studies have attempted to define the bond behaviour at the interface where premature failures originate [4-6]. Belarbi et al. [7] tested full-size RC T-beams in their experimental work on the shear behaviour of T-strengthened and full-size bridge beams to study the strengthening in shear with a FRP. In this study, the main investigated variables were the transverse steel reinforcement ratio and the effect of mechanical anchorage systems.

The shear strength of the FRP-strengthened beams was approximately 23% higher than that of the control beam without mechanical anchorages. Hamid et al. [8] tested simply supported concrete beams with either steel or glass FRP (GFRP) along their length. The study primarily focused on investigating the effects of shear span-effective depth ratios,

* Corresponding author: hussain.hasan2001m@coeng.uobaghdad.edu.iq

http://dx.doi.org/10.28991/CEJ-2023-09-10-04

longitudinal reinforcement ratios, and stirrup ratios. The results of the test were consistent with the predictions of the standard rules and design guidelines, except for the GFRP-RC beams, which failed in the stress test. Ozden et al. [9] conducted an experimental study to test 10 RC T-beams that were designed to have low shear strength. The study focused on investigating the significance of three main variables: the FRP material, the type of surface bonding, and the type of end anchorage for the strips. CFRP, GFRP, and high-elasticity modulus are all types of composite materials. The shear behaviour of the RC T-beams strengthened in shear by U-shaped FRP external stirrups was investigated. The type of surface bonding depended on whether the strips were fully or partially bonded to the surface of the beam. The partially bonded FRP strips did not have any surface bonding, but their ends near the slab-to-beam connection had epoxy-bonded FRP anchors. The ends of the strips with complete surface bonding either have FRP anchors glued together with epoxy or do not have any anchors. The test results showed that the design codes should be changed for Hi-Mod CFRP because the estimations of the existing codes consistently overestimate the increase in capacity. Meanwhile, the design codes typically overestimate the capability for situations without anchorage in FRP and Hi-Mod CFRP. This phenomenon could result in unsafe stress-stiffening applications.

Said et al. [10] presented an experimental and analytical study on the shear behaviour of concrete beams reinforced with lab-produced GFRP bars and stirrups. The bars and stirrups are made with local raw materials and a two-part die mould at the lab. Ten beams (120 wide, 300 deep, and 1550 mm long) were cast and tested under a four-point load until they broke. The main parameters were the compressive strength of the concrete and the vertical GFRP web reinforcement ratio, which were measured by the number of GFRP stirrups (8 @ 215, 8 @ 150, and 8 @ 100). The mid-span deflection, the load on the crack at an angle, and the strains in the GFRP reinforcement bars and stirrups were measured and compared for each tested beam. The test results showed that the shear capacities of a beam without stirrups increased by 41% and 82% when the web GFRP reinforcements of 8 @ 215 and 8 @ 100 were used, respectively. When the concrete's compressive strength increased from 25 MPa to 45 MPa to 70 MPa, the shear strength increased by 49% and 104%, respectively. The most strain that could be measured in the GFRP stirrups was 0.0095.

Issa et al. [11] investigated the shear strength and behaviour of concrete beams reinforced with basalt FRP bars with and without shear reinforcements. Six concrete beams of 200 × 300 mm (8 × 12 in) and 300 × 200 mm (12 × 8 in) were made with and without basalt FRP shear reinforcements. The flexural reinforcement ratios (ρ_f) of the non-shear-reinforced (NSR) concrete beams ranged from 2.69 to 14.8 times the balanced ratio (ρ_{fb}). The range of the shear-reinforced (SR) concrete beams was from 1.69 to 6.88 times the balanced ratio (ρ_{fb}). Two different shear span-to-depth (a/d) ratios (5.65 and 7.0) and three different a/d were considered (1.5, 2.5, and 3.5) for the NSR beams. The test results are shown in terms of crack patterns, ways the material broke, load deflection, load-strain behaviour, and shear strength. The shear capacity of the SR and NSR beams increased as the area of the basalt FRP reinforcement expanded, even though the span-to-depth ratio remained constant. When the span-to-depth ratio (a/d) increased, the shear capacity decreased.

The prediction models and design code equations were tested based on the experimental results to determine how well they could predict the shear strength of the basalt FRP RC beams. The conservative and non-conservative predictions were made with standard provisions. The forecasts were based on the changes. Fan et al. [12] conducted an experimental, theoretical, and numerical study of the shear behaviour of inorganic polymer concrete (IPC) beams reinforced with BFRP bars and stirrups, taking into account the effects of stirrup spacing (S = 80, 100, and 150 mm) and shear span-to-depth ratio (1.5, 2.0, and 2.5). The result indicated that all BFRP-IPC beams failed in shear because the BFRP stirrups broke, and the beams failed in shear and compression. Has a bigger effect on the shear performance of BFRP-reinforced IPC beams than S, reducing the ultimate shear load by 29.4%. The simulation results are consistent with the experimental data. Nonetheless, the existing design rules for FRP-RC did not consider this aspect. Consequently, the predictions did not match the experiments by more than 30%. Moreover, the modified equations were made, taking into account the effect.

Alwash et al. [13] examined 14 RC beams strengthened in shear by CFRP textiles bonded with cement-based adhesive CBA. The experimental results demonstrated that the CFRP textiles bonded with CBA substantially enhanced the shear capacity of the RC members. The structural performance of RC columns strengthened in shear with embedded through-section (ETS) GFRP bars has been experimentally and analytically investigated [14]. The results showed that the configuration and specifics of the anchorage system should be carefully considered prior to the formulation of unified specifications. Peng et al. [15] presented a comprehensive investigation of the shear behaviour of the RC beams reinforced with a small-diameter FRP bar-reinforced geopolymer matrix (FRGM) system. The findings indicated that utilising steel fibres in the geopolymer matrix further inhibited the formation of shear fractures and enhanced shear capacity.

According to the literature study that has been given above, and to our knowledge, no research studies were found studying the shear response of T-RC beams strengthened for shear using CFRP bars by the embedded through section (ETS) technique.

2. Research Significance

An experimental programme was carried out to examine the response of the RC T-beams strengthened by ETS. The programme aimed to investigate the effectiveness of the CFRP bars in improving the shear performance of the RC T-beams. Figure 1 shows a flowchart showing the methodology of this study.

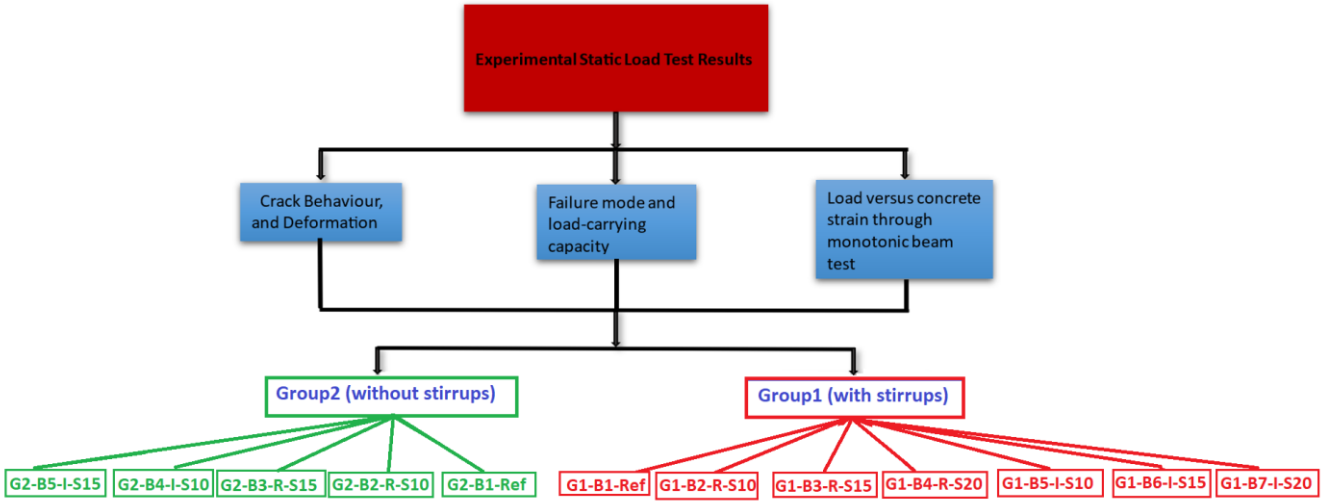

Figure 1. Flowchart of the research methodology

3. Experimental Programme and Material Properties

Twelve RC T beams were tested in the experimental programme, including two reference beams without any strengthening and ten strengthened beams. The twelve beams were divided into two main groups with and without stirrups (just three for steel bar support). The spacing and angle of inclination of the CFRP bars were the main variables. All strengthened beams were strengthened in shear with 12 mm CFRP bars inserted in the centre line of the section with different spacings and angles of inclination. The experimental analysis was performed to study the effect of spacing and angle of inclination of the CFRP bars on the failure load, crack distribution, load-strain relationships, and load-deflection relationships. The beams of every group have the same length (2200 mm), cross-sectional dimensions, and reinforcement. All beams were subjected to a monotonic one-point load at mid-span till failure, as shown in Figures 2 and 3. The tested beams were designed according to ACI-318-19 [16] and ACI440.2R-17 [17]. Table 1 illustrates the configuration and designation of the tested beams.

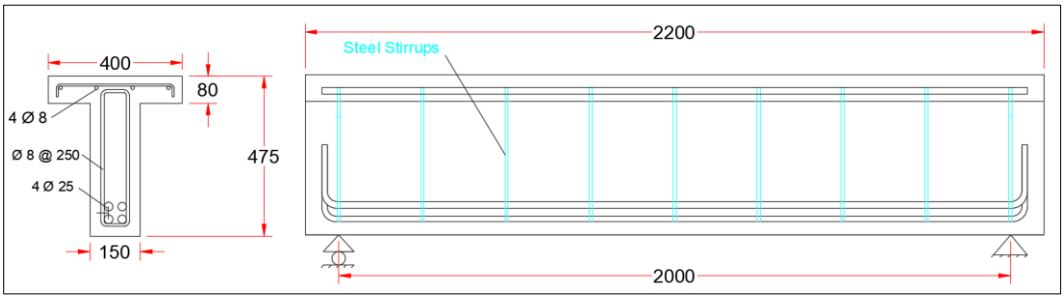

a. Reference beam (un-strengthened)

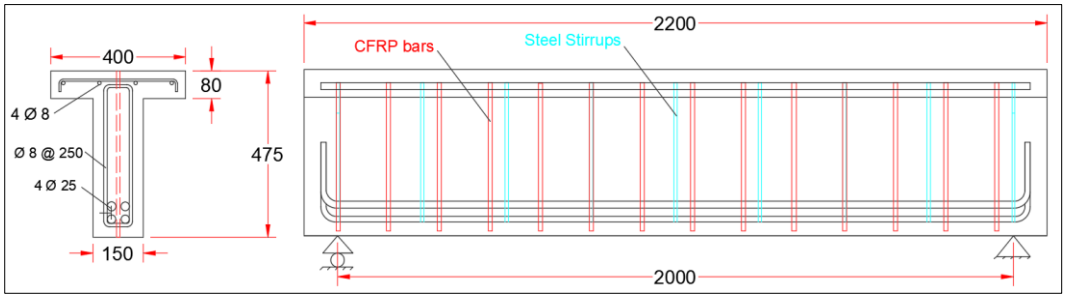

b. Strengthened beam

Figure 2. Details of the beams for group one (with stirrups) (all dimensions are in mm)

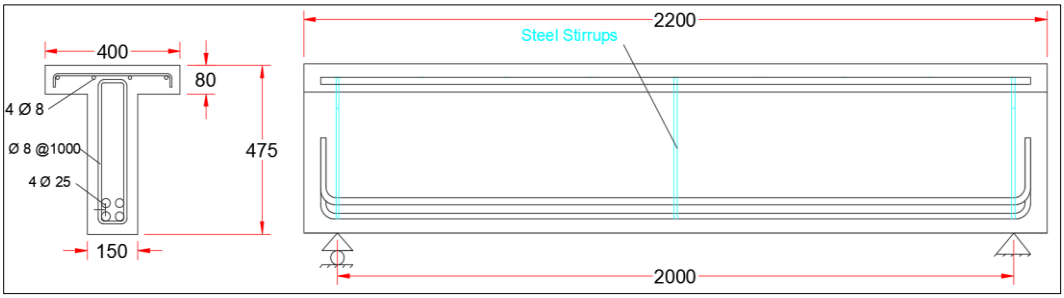

a. Reference beam (un-strengthened)

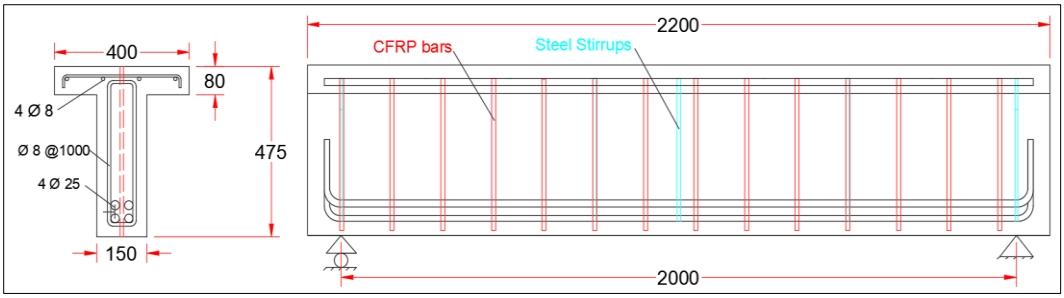

b. Strengthened beam

Figure 3. Details of the beams for group two without stirrups (just three for support) (all dimensions are in mm)

Table 1. Details of the examined beams

Group	Beam-ID	Angle of inclination of CFRP bar (degree)	CFRP bar spacing (cm)
Group one with stirrups	G1-B1-Ref	–	–
	G1-B2-R-S10	90	10
	G1-B3-R-S15	90	15
	G1-B4-R-S20	90	20
	G1-B5-I-S10	45	10
	G1-B6-I-S15	45	15
	G1-B7-I-S20	45	20
Group two without stirrups	G2-B1-Ref	–	–
	G2-B2-R-S10	90	10
	G2-B3-R-S15	90	15
	G2-B4-I-S10	45	10
	G2-B5-I-S15	45	15

Concrete's properties, such as its modulus of elasticity, tensile strengths, and compressive strengths, were calculated using steel cylinder moulds that were 15 cm in diameter and 30 cm in height, or cubes of 15 × 15 × 15 cm. Standard bar tests were conducted to evaluate the mean yield strength and ultimate stress of the reinforcing steel bars. The properties of the concrete (after 28 days) and the steel reinforcements employed in this study are illustrated in Table 2. Table 3 provides the sieve analysis of the sand, and Table 4 illustrates the coarse aggregate grading used in this study. The characteristics of the CFRP bars are shown in Table 5.

Table 2. Material's properties

Material	Splitting tensile strengths (MPa)	Compressive strength fcu (MPa)	Yield stresses (MPa)	Ultimate tensile strengths (MPa)	Elasticity modulus (GPa)
Concrete.	3.73	45.3	–	–	28.645
Steel Ø8 mm	–	–	523	662	200
Steel Ø25 mm	–	–	572.4	724.9	200

Table 3. Sieve analysis (grading) of the used fine aggregate

Sieve size (mm)	Passing % by weight	Limits of the Iraqi Specification No. 45/1984 Zone 2
10.0	100	100
4.750	91	90–100
2.360	76	75–100
1.180	63	55–90
0.600	51	35–55
0.300	22.5	8–30
0.15	7.9	0–10

Table 4. Grading of the coarse aggregate

Sieve size (mm)	Cumulative passing (%)	IQS. No.45/1984, Grade 5-20 mm
75.0	100	–
63.0	100	–
37.5	100	100
20	95	95-100
14	–	–
10	31	30-60
5	1	0–10
2.36	–	–

Table 5. Mechanical properties of the CFRP bars

Product name	Sika® CarboDur® BC rods
Tensile strengths (MPa)	3100
E-modulus (GPa)	148
Breaking strain (min, %)	1.70
Diameter (mm)	12
Weight (kg/m)	≤0.32

4. Static Load Test Results

The test results and behaviour of the strengthened specimens were compared with those of the un-strengthened control T-beams for two groups (with and without stirrups), and the effects of spacing and angle of inclination of the CFRP bars of shear strength were discussed.

4.1. Initial Crack Load and Pattern

The experimental results concerning cracking and failure loads are shown in Table 6. The initial flexural crack occurred within a load range of 60 kN to 80 kN with a different first crack load (Pcr)/ultimate load (Pu) percent ranging from 11.2% to 14.5% for the beams of group one. By contrast, the first flexural crack occurred at the applied load ranging from 50 kN to 80 kN with a different first crack load (Pcr)/ultimate load (Pu) percent (11.8% to 22.6%) for the beams of group two. The (Pcr/Pu) percent values for all beams were close, except for the beam without CFRP or shear stirrups, which were high. The result showed that the effect of the CFRP bars on the Pcr/Pu percent was small in the elastic stage. The (Pcr/Pu) percent value of the control beam (without CFRP bars) was high (22.6%) because concrete alone bears tensile stresses in this beam. Figures 4 and 5 show the load and deflection at the cracking and ultimate stages, respectively, for all beams.

Table 6. Crack and ultimate loads of all the beams

Group	Specimens	Cracking load (Pcr) (kN)	Deflection at cracking load (δcr) (mm)	% increase in the cracking load concerning ref. of every group	Ultimate loads (Pu) (kN)	Pcr/Pu (%)
Group one (with stirrups)	G1-B1-Ref	60	1.35	Ref.	451	13.3
	G1-B2-R-S10	80	1	33	570	14
	G1-B3-R-S15	60	1.01	0	535	11.2
	G1-B4-R-S20	60	1.15	0	501	12
	G1-B5-I-S10	80	0.94	33	585	13.7
	G1-B6-I-S15	80	1.09	33	552	14.5
	G1-B7-I-S20	70	1.21	17	521	13.4
Group two (without stirrups)	G2-B1-Ref	50	1.3	Ref.	221	22.6
	G2-B2-R-S10	80	1.18	60	519	15.4
	G2-B3-R-S15	80	1.31	60	502	16
	G2-B4-I-S10	70	0.93	40	532	13.2
	G2-B5-I-S15	60	1.1	20	510	11.8

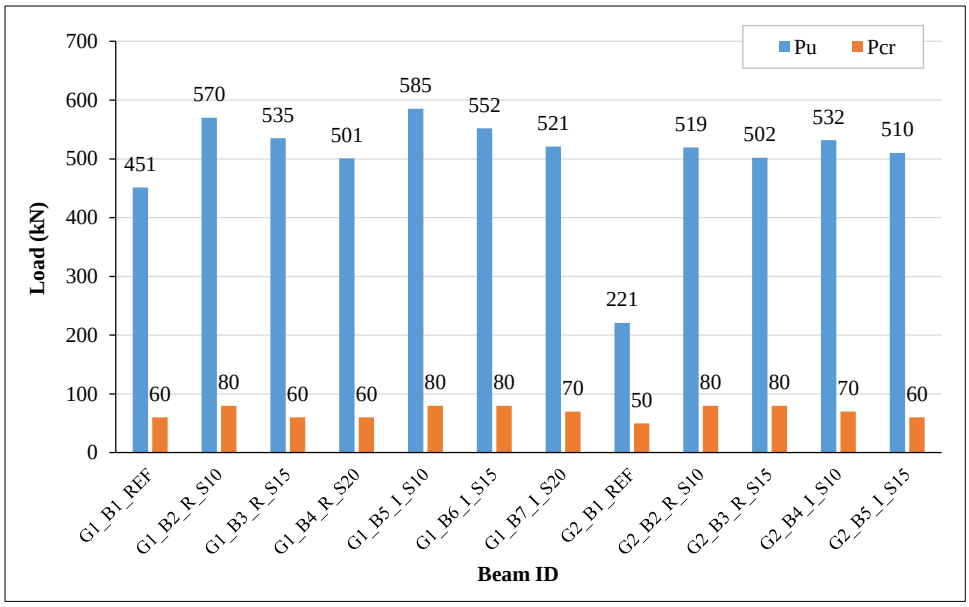

Figure 4. Load at the cracking and ultimate stages of all beams

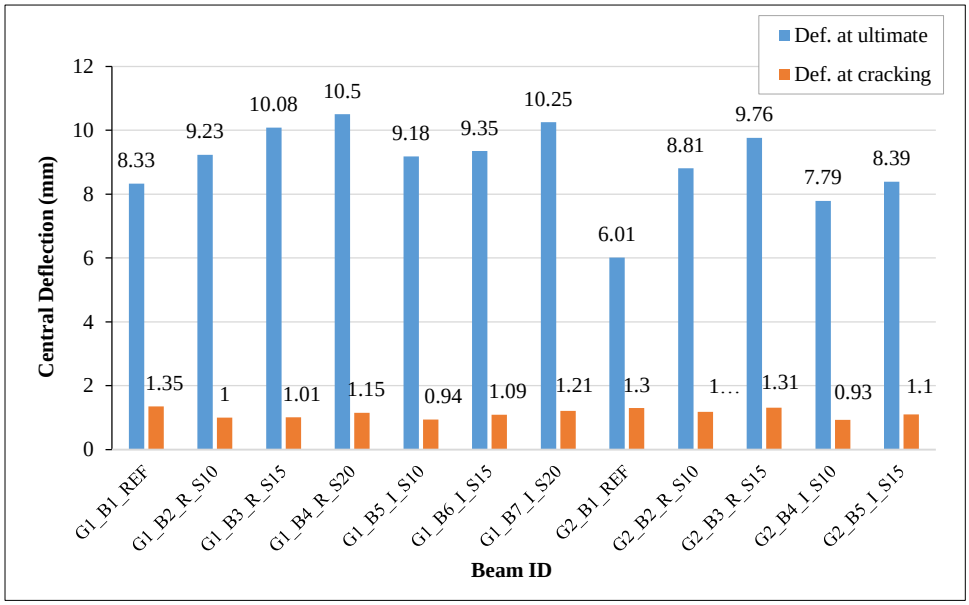

Figure 5. Deflection at the cracking and ultimate loads of all beams

Diagonal tension failure was observed for all the RC-tested beams. This failure occurred due to the diagonal shear crack quickly extending towards the load point after it was initiated. The control beams failed to shear, as evident from the diagonal shear cracks on both shear spans. The strengthening beams with CFRP bars resulted in the delayed appearance of the first cracks for the diagonal and flexure cracks, and the diagonal cracks appeared before the flexure cracks due to the preliminary design of the beams, which are deemed to fail in shear rather than flexure.

4.2. Load–Deflection Curves

Deformability can refer to the strain in a body, the curvature in a section, a member's rotation, and a member's deflection. Figures 6 and 7 show the relationships between the applied load and the mid-span deflection from the start of the loadings to the failure stage for the T-beams of groups one and two, respectively. The data shown in the figures ended at the failure load and its corresponding deflection value because the load behaviour could not be regulated after the peak in all tested beams.

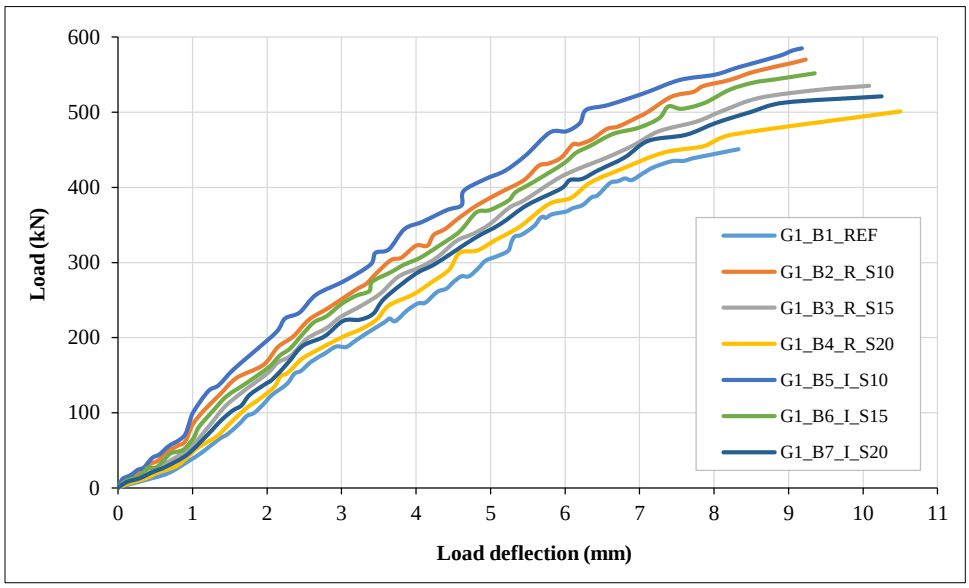

Figure 6. Load–deflection curves of group one (with stirrups)

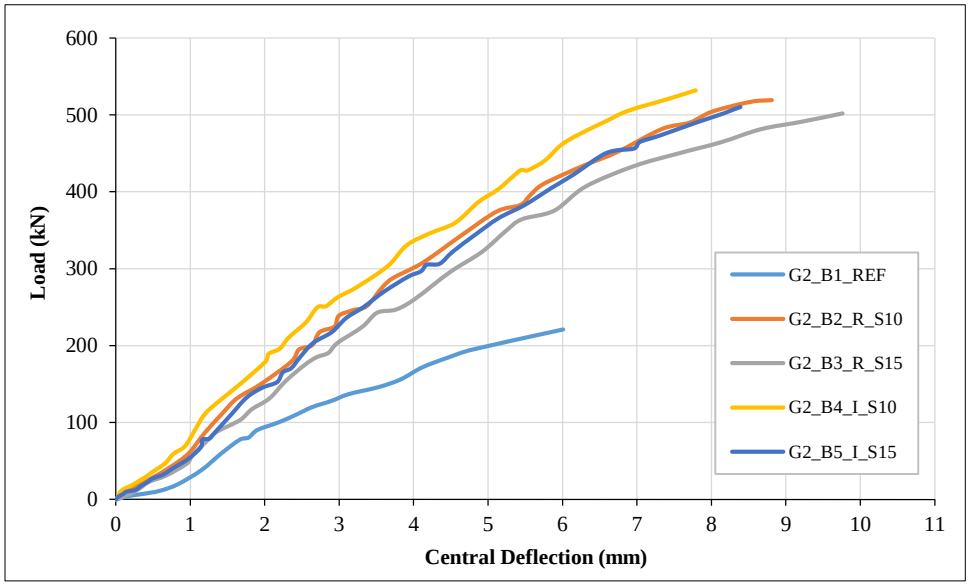

Figure 7. Load–deflection curves of group two (without stirrups)

Several researchers, such as Mansur et al. [18], asserted that the final trial load split by 1.7 was the serviceability limit. This value was selected to ensure that no undesired breaking or distortion occurred at this point. Tables 7 and 8 summarise the relevant mid-span deflections for the loading stages of service load, the ultimate load of the reference beam of every group, and the ultimate applied load for each beam for groups one and two, respectively. The selection of the ultimate load of the reference beam of the group is essential to comparing deflections at a constant load.

Table 7. Load and the corresponding deflection of group one at different loading stages

Beam ID	At service loading Ps		At 451 kN		At ultimate load		Failure load P_{ult} (kN)
	Deflection (mm)	Percentage of decrease (%)	Deflection (mm)	Percentage of decrease (%)	Deflection (mm)	Percentage of increase (%)	
G1-B1-Ref	4.5	Ref.	8.33	Ref.	8.33	Ref.	451
G1-B2-R-S10	4.22	6.2	6.05	27.4	9.23	10.8	570
G1-B3-R-S15	4.4	2.2	6.9	17.2	10.08	21	535
G1-B4-R-S20	4.49	0.22	7.86	5.6	10.5	26	501
G1-B5-I-S10	3.85	14.4	5.62	32.5	9.18	10.2	585
G1-B6-I-S15	4.31	4.2	6.33	24	9.35	12.2	552
G1-B7-I-S20	4.45	1.1	7.01	15.9	10.25	23	521

Table 8. Load and the corresponding deflection of group two at different loading stages

Beam ID	At service loading Ps		At 221 kN		At ultimate load		Failure load P_{ult} (kN)
	Deflection (mm)	Percentage of increasing (%)	Deflection (mm)	Percentage of decreasing (%)	Deflection (mm)	Percentage of increasing (%)	
G2-B1-Ref	2.9	Ref.	6.01	Ref.	6.01	Ref.	221
G2-B2-R-S10	4.12	42	2.8	53	8.81	47	519
G2-B3-R-S15	4.48	55	3.2	47	9.76	62	502
G2-B4-I-S10	3.8	31	2.4	60	7.79	30	532
G2-B5-I-S15	4.14	43	2.91	52	8.39	40	510

When a beam was incrementally loaded, the deflection increased at a constant rate (elastic region) at the initial stage. After the cracking load, the investigated beams continued to deflect in a semi-linear fashion with load, and the deflection curves diverged from each other based on the level of cracking that was achieved and the degree to which the beam's stiffness had degraded. The angle at which this linear portion was angled was not consistent across all specimens from the same group. When loads are brought close to the ultimate load, the tested beams begin to roughly nonlinearly deflect with load, resulting in deflection curves that are markedly different from the deflection curve of the reference beam of every group.

According to the recommended maximum permissible deflection by ACI-318M-19 [16] (L/180 = 11.11 mm) for flat roofs not supporting or attached to the non-structural elements likely to be damaged by large deflections, Tables 5 and 6 show that all tested beams did not exceed this limit at service load.

At the stage of service load, the mid-span deflection of the reference beam of group one (with stirrups) decreased by 6.2%, 2.2%, 0.22%, 14.4%, 4.2%, and 1.1% for G1-B2-R-S10, G1-B3-R-S15, G1-B4-R-S20, G1-B5-I-S10, G1-B6-I-S15, and G1-B7-I-S20, respectively. Meanwhile, the mid-span deflection of the reference beam in group two (without stirrups) increased by 42%, 55%, 31%, and 43% for G2-B2-R-S10, G2-B3-R-S15, G2-B4-I-S10, and G2-B5-I-S15, respectively.

At a load equal to the ultimate load of the reference beam of group one (451 kN), the mid-span deflection decreases by 27.4, 17.2, 5.6, 32.5, 24, and 15.9% for G1-B2-R-S10, G1-B3-R-S15, G1-B4-R-S20, G1-B5-I-S10, G1-B6-I-S15, and G1-B7-I-S20, respectively, for group one [with stirrups] concerning the reference beam. This means that the existing CFRP bars increase the shear stiffness of the beam.

At the load equal to the ultimate load of the reference beam of group two (221 kN), the mid-span deflection of the reference beam of group two (without stirrups) decreased by 53%, 47%, 60%, and 52% for G2-B2-R-S10, G2-B3-R-S15, G2-B4-I-S10, and G2-B5-I-S15, respectively. This result means that the existing of CFRP bars increased the shear stiffness of the beam.

At the ultimate load, the mid-span deflection of the reference beam in group one (with stirrups) increased by 10.8%, 21%, 26%, 10.2%, 12.2%, and 23% for G1-B2-R-S10, G1-B3-R-S15, G1-B4-R-S20, G1-B5-I-S10, G1-B6-I-S15, and G1-B7-I-S20, respectively. Meanwhile, the mid-span deflection of the reference beam in group two (without stirrups) increased by 47%, 62%, 30%, and 40% for G2-B2-R-S10, G2-B3-R-S15, G2-B4-I-S10, and G2-B5-I-S15, respectively.

4.2.1. Effect of Spacing of the CFRP Bars

The effect of the spacing of the CFRP bars on the load-deflection behaviour at mid-span is illustrated in Figures 8 to 11. The results for group one are compared with this group's control specimen (without CFRP). According to the load-deflection relationships, the beams have the same stiffness in the elastic region, whereas the increasing spacing of the CFRP bars after cracking is inversely proportional to the beam stiffness for the exact angle of inclination or the deflection increase at the same load level, as shown in Figures 7 and 8.

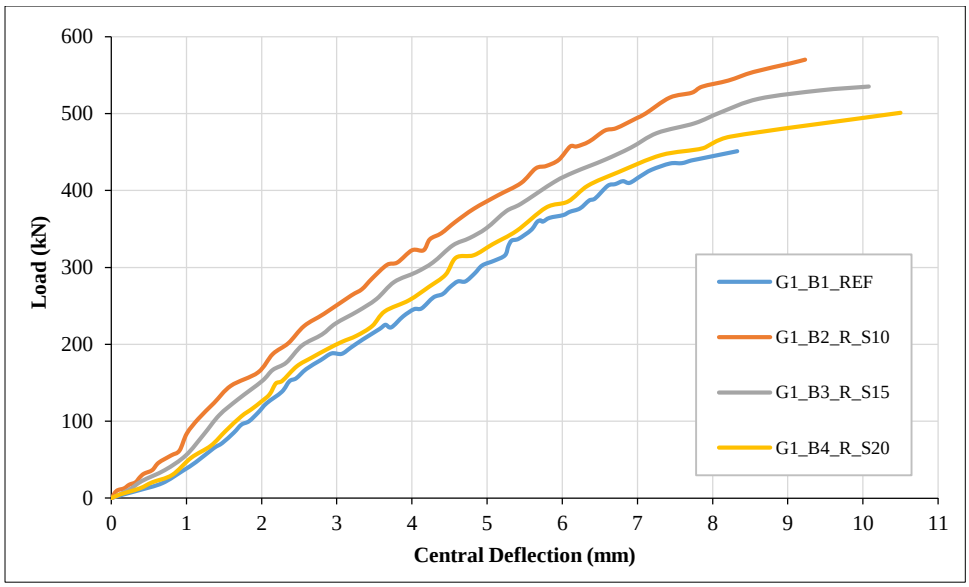

Figure 8. Load–deflection curves of the beams of group one with vertical CFRP bars

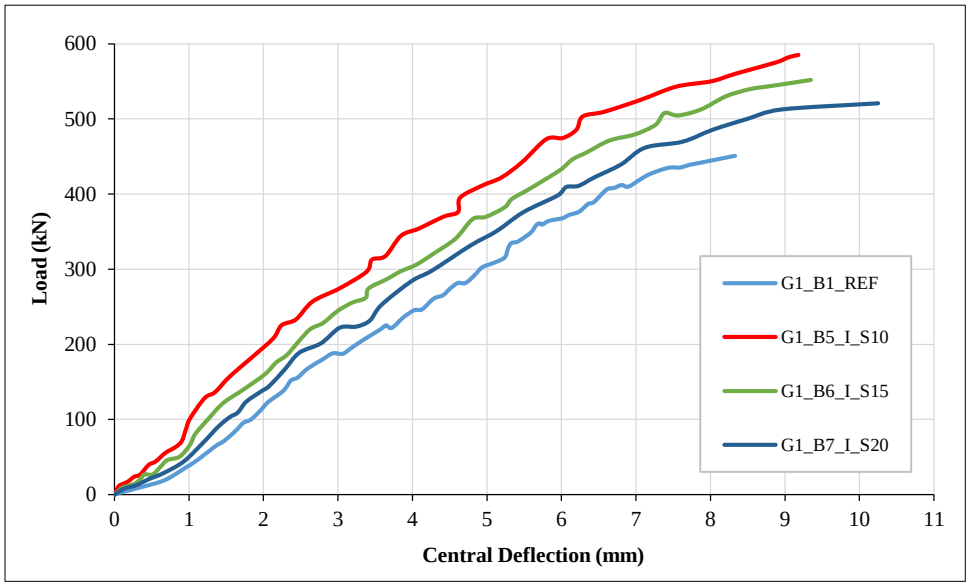

Figure 9. Load–deflection curves of the beams of group one with inclined CFRP bars

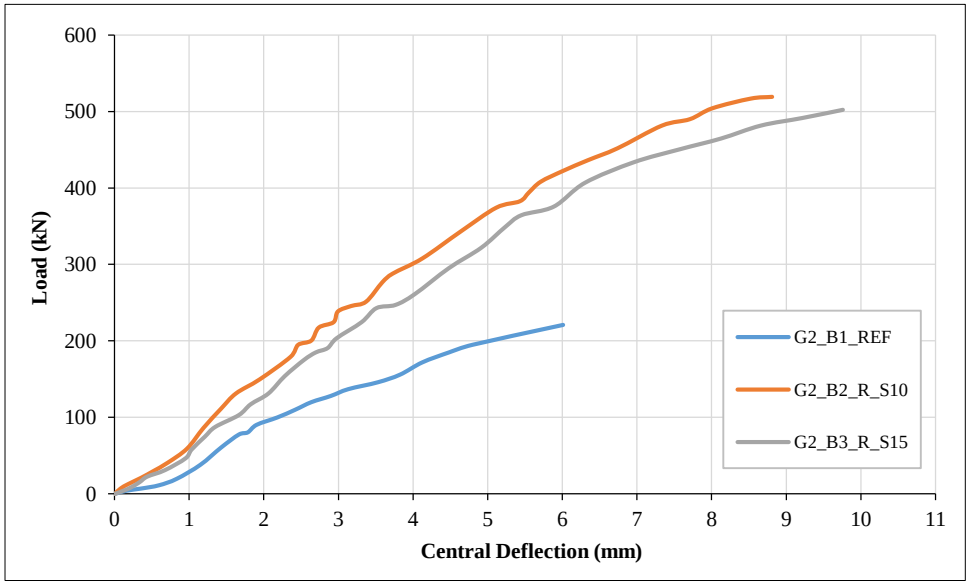

Figure 10. Load–deflection curves of the beams of group two with vertical CFRP bars

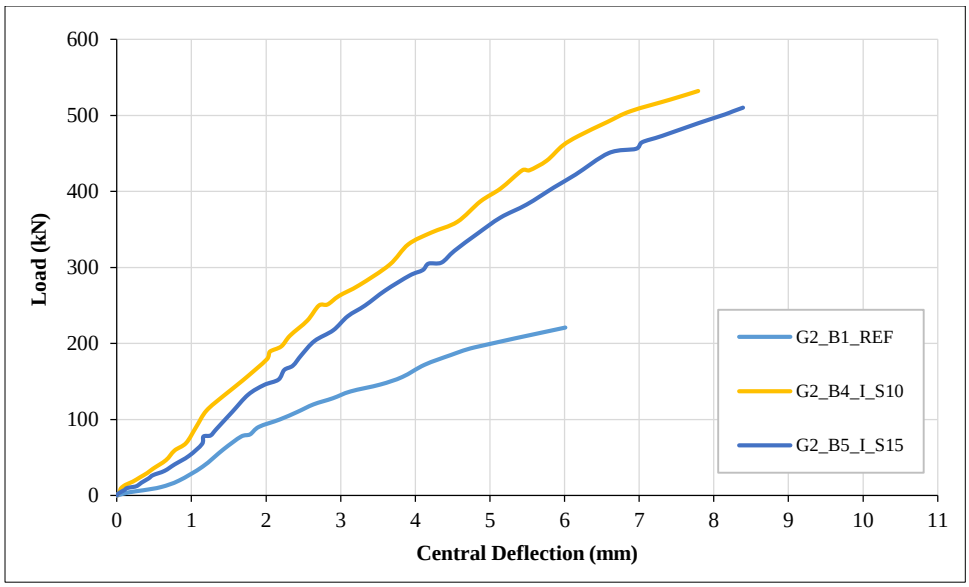

Figure 11. Load–deflection curves of the beams of group two with inclined CFRP bars

In Table 5, the mid-span deflection of the beams of group one with vertical CFRP bars and at a load equal to the ultimate load of the reference beam (451 kN) decreased by 27.4, 17.2, and 5.6% for the beams with CFRP bar spacings of 10, 15, and 20 cm, respectively. Moreover, the mid-span deflection of the beams of group one with inclined CFRP bars (45°) and at a load equal to the ultimate load of the reference beam of group one (451 kN) decreased by 32.5%, 24%, and 15.9% for the beams with CFRP bar spacings of 10, 15, and 20 cm, respectively. This result means that the increasing spacing of the CFRP bars is inversely proportional with the beam stiffness for the exact angle of inclination.

In Table 6, the mid-span deflection of the reference beams of group two with vertical CFRP bars and at a load equal to the ultimate load of the reference beam of group two (221 kN) decreased by 53% and 47% for the beams with CFRP bar spacings of 10 and 15 cm, respectively. Moreover, the mid-span deflection of the reference beams of group two with inclined CFRP bars (45°) and at a load equal to the ultimate load of the reference beam of group two (221 kN) decreased by 60% and 52% for the beams with CFRP bar spacings of 10 and 15 cm. This result means that the increasing spacing of the CFRP bars is inversely proportional with beam stiffness for the same angle of inclination. The aforementioned result supports the findings of Rashmi et al. [19].

4.2.2. Effect of Angle of Inclination of the CFRP Bars

The effect of the angle of inclination of the CFRP bars on the load-deflection behaviour at mid-span is illustrated in Figures 12 to 14. Every figure has beams with the same spacing as the CFRP bars. The beams with inclined CFRP bars (45°) exhibited shear stiffness higher than those with vertical CFRP bars (90°) with a similar spacing. This result supports the findings of Van Hong Bui et al. [20]. The beam from group one (with stirrups) has higher shear stiffness than the similar beam from group two (without stirrups).

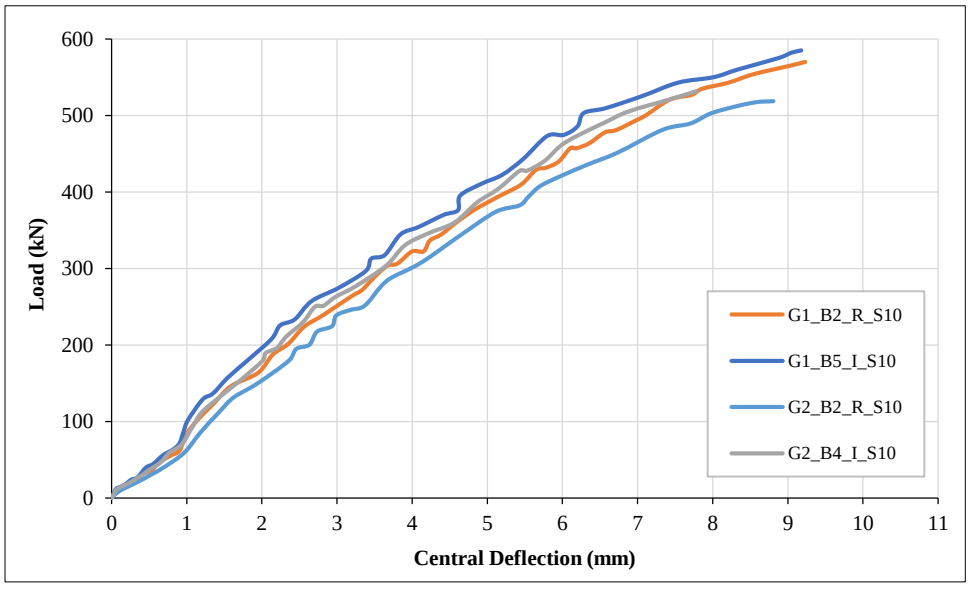

Figure 12. Load–deflection curves of the beams with a CFRP bar spacing of 10 cm

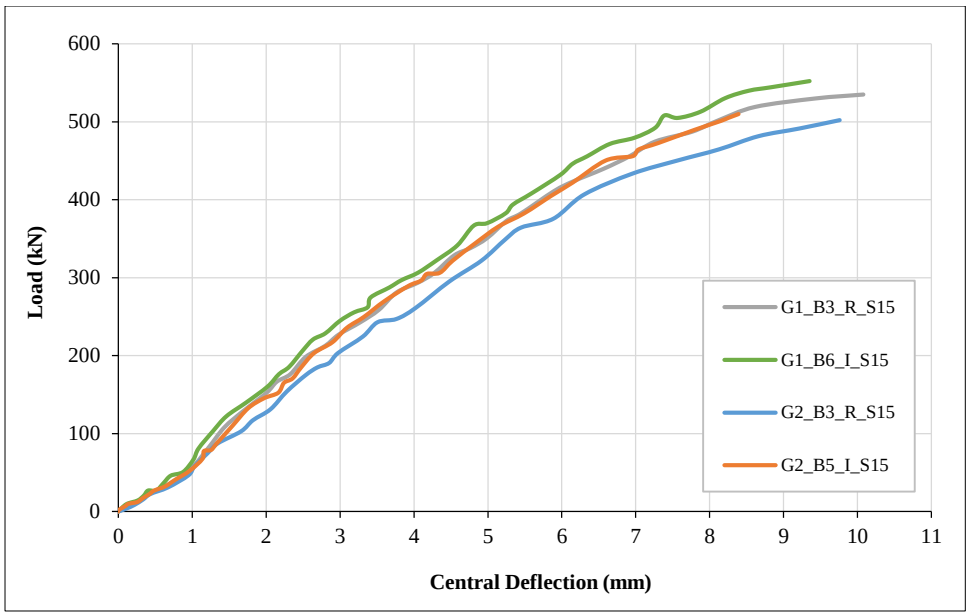

Figure 13. Load–deflection curves of the beams with a CFRP bar spacing of 15 cm

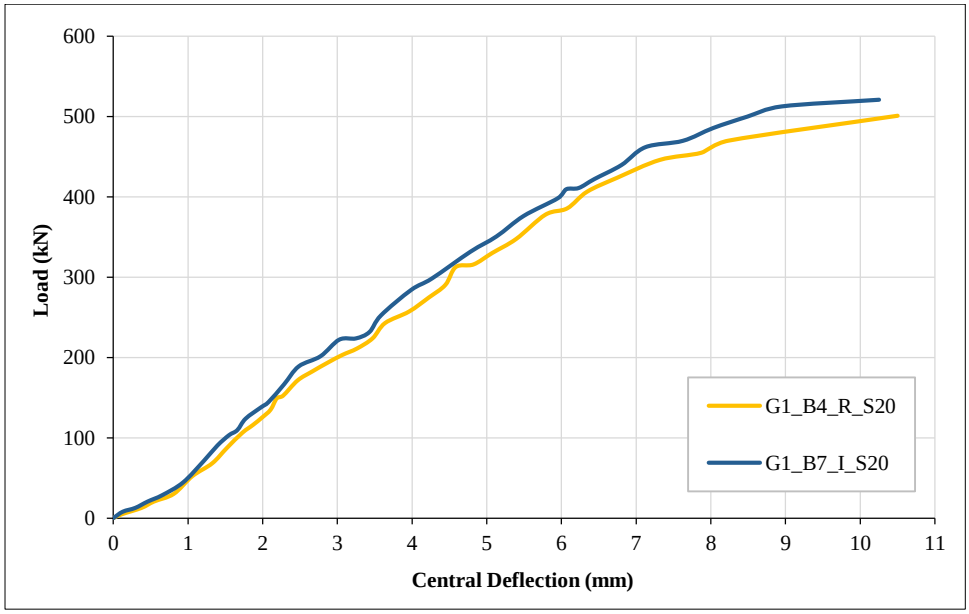

Figure 14. Load–deflection curves of the beams with a CFRP bar spacing of 20 cm

In group one (with stirrups), the beams with inclined CFRP bars (45°) and a spacing of 10 cm have shear stiffness slightly higher than those with vertical CFRP bars (90°) with a similar spacing. The mid-span deflection decreases by 8.8%, 7.1%, and 0.5% at the service load (451 kN) and ultimate load, as shown in Table 9.

Table 9. Load and the corresponding deflection of the beams of group one with a CFRP bar spacing of 10 cm at different loading stages

Beam ID	At service loading Ps		At 451 kN		At ultimate load		Failure load P_{ult} (kN)
	Deflection (mm)	Percentage of decrease (%)	Deflection (mm)	Percentage of decrease (%)	Deflection (mm)	Percentage of decrease (%)	
G1-B2-R-S10	4.22	Ref.	6.05	Ref.	9.23	Ref.	570
G1-B5-I-S10	3.85	8.8	5.62	7.1	9.18	0.5	585

In group two (without stirrups), the beams with inclined CFRP bars (45°) and a spacing of 10 cm have shear stiffness slightly higher than those with vertical CFRP bars (90°) with a similar spacing. The mid-span deflection decreased by 7.8%, 14.3% and 11.6% at service load (221 kN) and ultimate load, as shown in Table 10.

Table 10. Load and the corresponding deflection of the beams of group two with a CFRP bar spacing of 10 cm at different loading stages

Beam ID	At service loading Ps		At 221 kN		At ultimate load		Failure load P_{ult} (kN)
	Deflection (mm)	Percentage of increase (%)	Deflection (mm)	Percentage of decrease (%)	Deflection (mm)	Percentage of increase (%)	
G2-B2-R-S10	4.12	Ref.	2.8	Ref.	8.81	Ref.	519
G2-B4-I-S10	3.8	7.8	2.4	14.3	7.79	11.6	532

In group one (with stirrups), the beam with inclined CFRP bars (45°) and a spacing of 15 cm has shear stiffness slightly higher than that with vertical CFRP bars (90°) with a similar spacing where the mid-span deflection decreased by 2%, 8.3% and 7.2% at service load (451 kN) and ultimate load, as shown in Table 11.

Table 11. Load and the corresponding deflection of the beams of group one with a CFRP bar spacing of 15 cm at different loading stages

Beam ID	At service loading Ps		At 451 kN		At ultimate load		Failure load P_{ult} (kN)
	Deflection (mm)	Percentage of decrease (%)	Deflection (mm)	Percentage of decrease (%)	Deflection (mm)	Percentage of decrease (%)	
G1-B3-R-S15	4.4	Ref.	6.9	Ref.	10.08	Ref.	535
G1-B6-I-S15	4.31	2	6.33	8.3	9.35	7.2	552

In group two (without stirrups), the beam with inclined CFRP bars (45°) and a spacing of 15 cm has shear stiffness slightly higher than that with vertical CFRP bars (90°) with a similar spacing. The mid-span deflection decreased by 7.6%, 9% and 14% at service load (221 kN) and ultimate load, as shown in Table 12.

Table 12. Load and the corresponding deflection of the beams of group two with a CFRP bar spacing of 15 cm at different loading stages

Beam ID	At service loading Ps		At 221 kN		At ultimate load		Failure load P_{ult} (kN)
	Deflection (mm)	Percentage of increase (%)	Deflection (mm)	Percentage of decrease (%)	Deflection (mm)	Percentage of increase (%)	
G2-B3-R-S15	4.48	Ref.	3.2	Ref.	9.76	Ref.	502
G2-B5-I-S15	4.14	7.6	2.91	9	8.39	14	510

In group one (with stirrups), the beam with inclined CFRP bars (45°) and a spacing of 20 cm has shear stiffness slightly higher than that with vertical CFRP bars (90°) with a similar spacing. The mid-span deflection decreased by 0.9%, 10.8% and 2.4% at service load (451 kN) and ultimate load, as shown in Table 13.

Table 13. Load and the corresponding deflection of the beams of group one with a CFRP bar spacing of 20 cm at different loading stages

Beam ID	At service loading Ps		At 451 kN		At ultimate load		Failure load P_{ult} (kN)
	Deflection (mm)	Percentage of decreasing (%)	Deflection (mm)	Percentage of decreasing (%)	Deflection (mm)	Percentage of decreasing (%)	
G1-B4-R-S20	4.49	Ref.	7.86	Ref.	10.5	Ref.	501
G1-B7-I-S20	4.45	0.9	7.01	10.8	10.25	2.4	521

4.3. Failure Mode and Ultimate Load

According to the findings of this investigation, the failure load is defined as the load equivalent to the greatest static load applied above which the beam had a significant decrease in its strength and ultimately failed.

Failure in shear occurs when a beam has a shear resistance that is lower than its flexural strength and the shear force applied to the beam is greater than the shear capacity of the various materials that make up the beam. A force that has the tendency to cause a sliding failure on a material along a plane that is parallel to the direction in which the force is acting is known as the shear load.

Shear failure caused diagonal tensile fractures in each and every one of the beams. The control samples and the enhanced samples made with CFRP bars exhibited shear cracks that were dispersed over the shear span. The shear cracks continued to spread higher through the flange and closer to the loading point with the application of load. Failure of the

reinforced specimens occurred immediately after the CFRP bars that had intercepted the diagonal shear fractures were deboned. Consequently, the point at which steel stirrups yield under greater applied stresses was significantly pushed back when the reinforced specimens were considered. The failure manner and fracture patterns of the T-beams are shown in Figures 15 to 26, which may be found below.

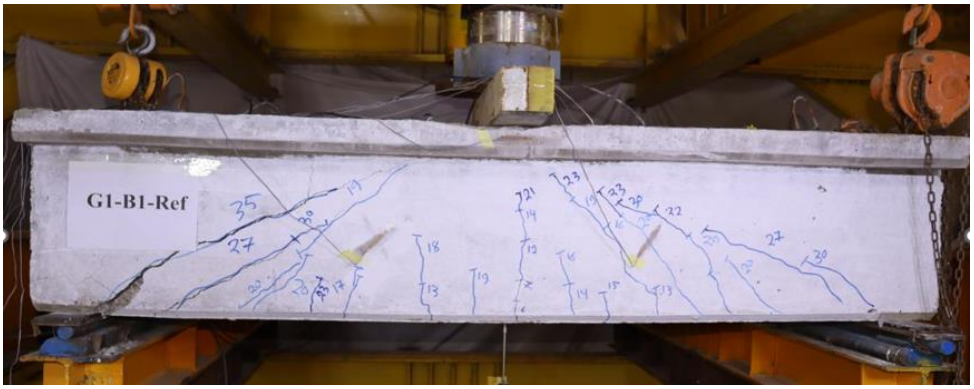

Figure 15. Failure crack pattern of specimen G1-B1-REF

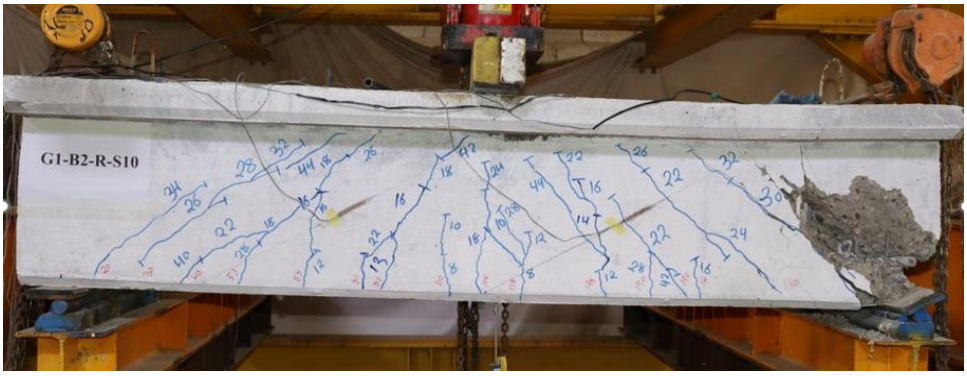

Figure 16. Failure crack pattern of specimen G1-B2-R-S10

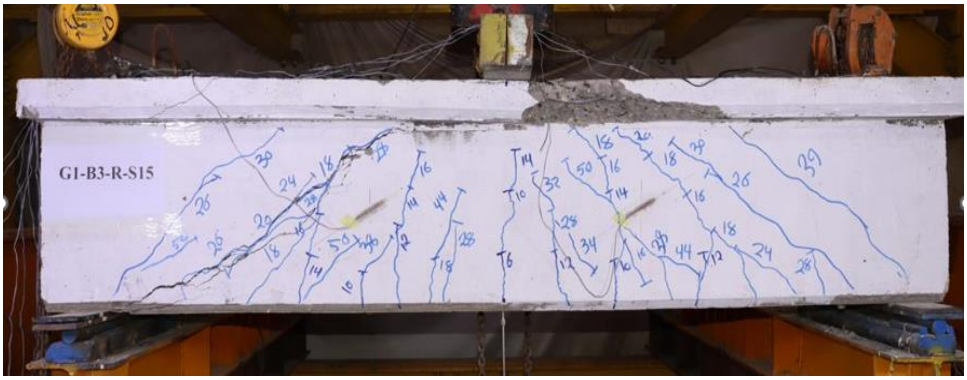

Figure 17. Failure crack pattern of specimen G1-B3-R-S15

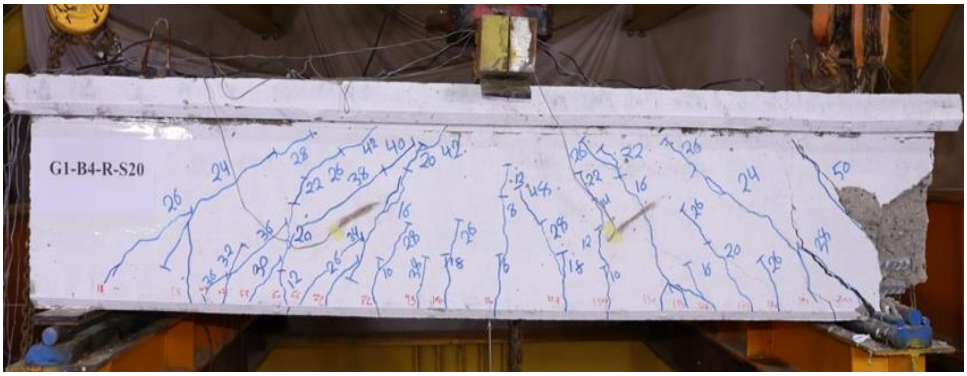

Figure 18. Failure crack pattern of specimen G1-B4-R-S20

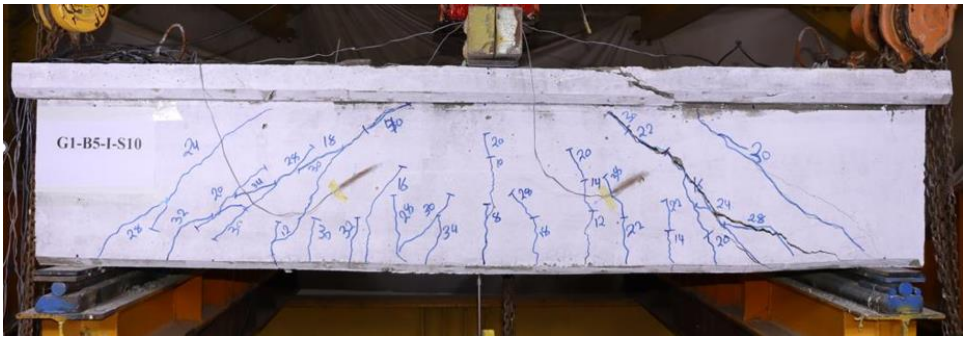

Figure 19. Failure crack pattern of specimen G1-B5-I-S10

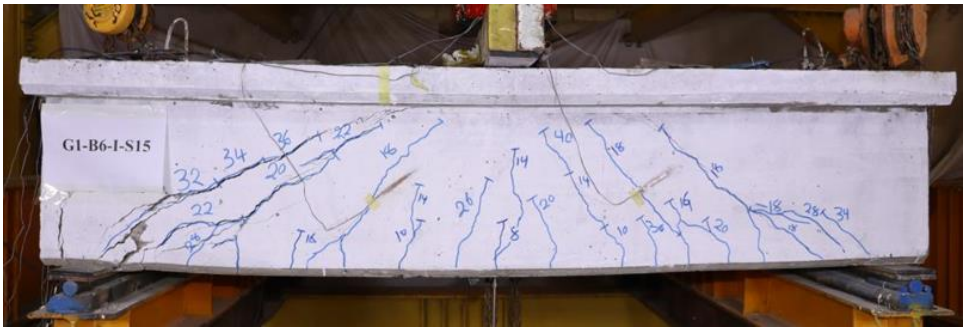

Figure 20. Failure crack pattern of specimen G1-B6-I-S15

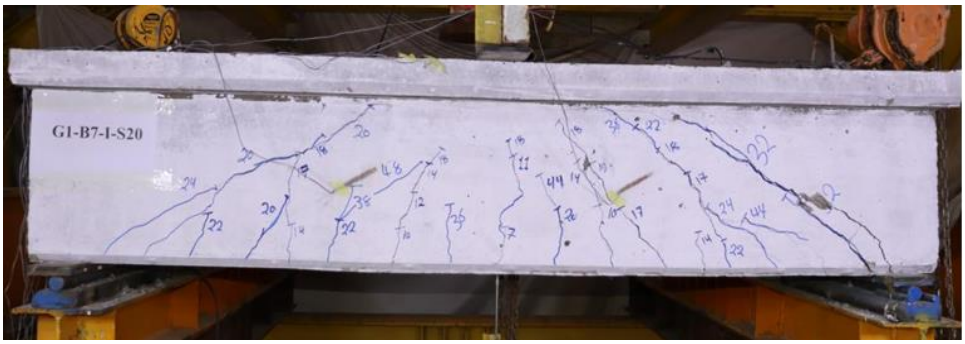

Figure 21. Failure crack pattern of specimen G1-B7-I-S20

Figure 22. Failure crack pattern of specimen G2-B1-REF

Figure 23. Failure crack pattern of specimen G2-B2-R-S10

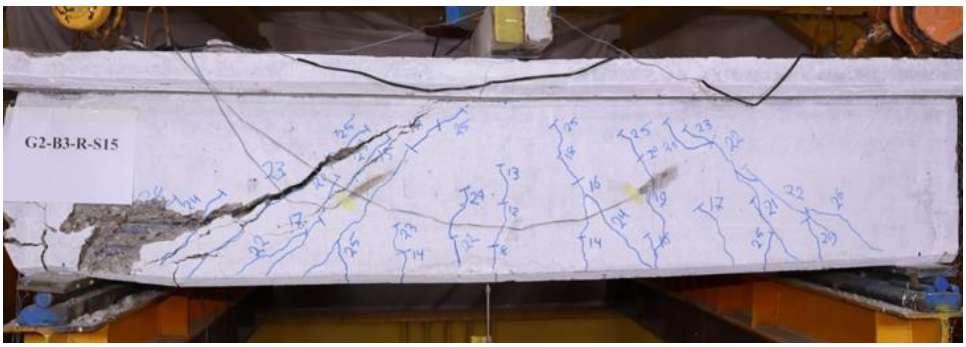

Figure 24. Failure crack pattern of specimen G2-B3-R-S15

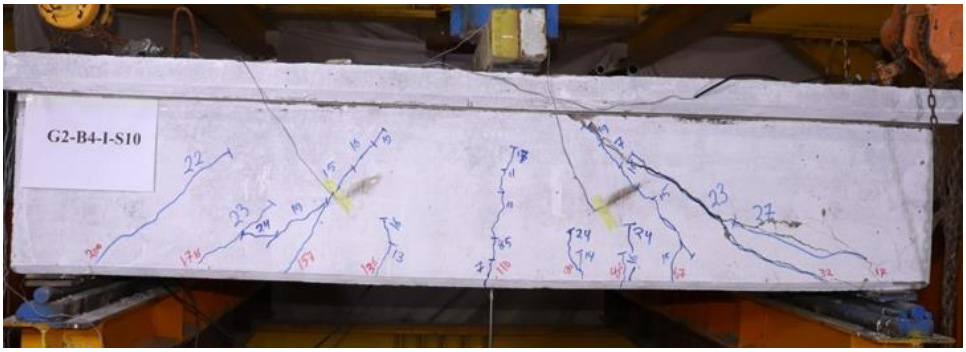

Figure 25. Failure crack pattern of specimen G2-B4-I-S10

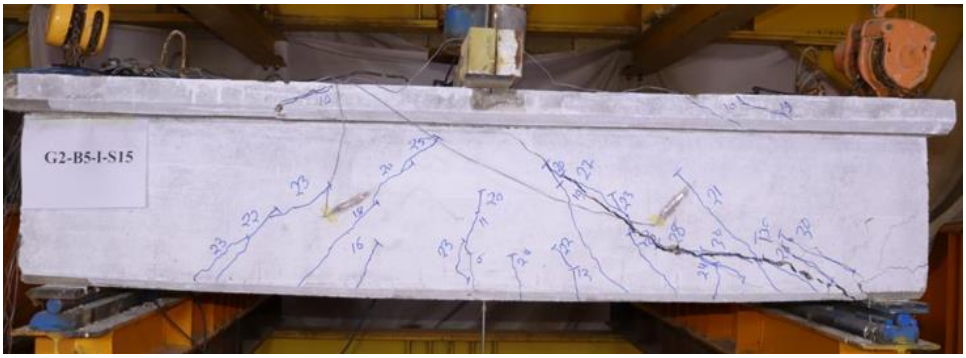

Figure 26. Failure crack pattern of specimen G2-B5-I-S15

Table 14 shows that the ultimate load of the reference beam of group one (with stirrups) increased by 26.4%, 18.6%, 11.1%, 29.7%, 22.4%, and 15.5% for G1-B2-R-S10, G1-B3-R-S15, G1-B4-R-S20, G1-B5-I-S10, G1-B6-I-S15, and G1-B7-I-S20, respectively. Meanwhile, the ultimate load of the reference beam increased in group two (without stirrups) by 135%, 127%, 141%, and 131% for G2-B2-R-S10, G2-B3-R-S15, G2-B4-I-S10, and G2-B5-I-S15, respectively.

Table 14. Ultimate loads of all beams

Group	Specimens	Ultimate load (Pu) (kN)	% increase in the ultimate load concerning ref. of every group
Group 1 (with stirrups)	G1-B1-Ref	451	Ref.
	G1-B2-R-S10	570	26.4
	G1-B3-R-S15	535	18.6
	G1-B4-R-S20	501	11.1
	G1-B5-I-S10	585	29.7
	G1-B6-I-S15	552	22.4
	G1-B7-I-S20	521	15.5
Group 2 (without stirrups)	G2-B1-Ref	221	Ref.
	G2-B2-R-S10	519	135
	G2-B3-R-S15	502	127
	G2-B4-I-S10	532	141
	G2-B5-I-S15	510	131

The CFRP bars were more effective in group two in than group one because the beams of group two do not have shear stirrups. Figure 27 shows the ultimate load of all beams.

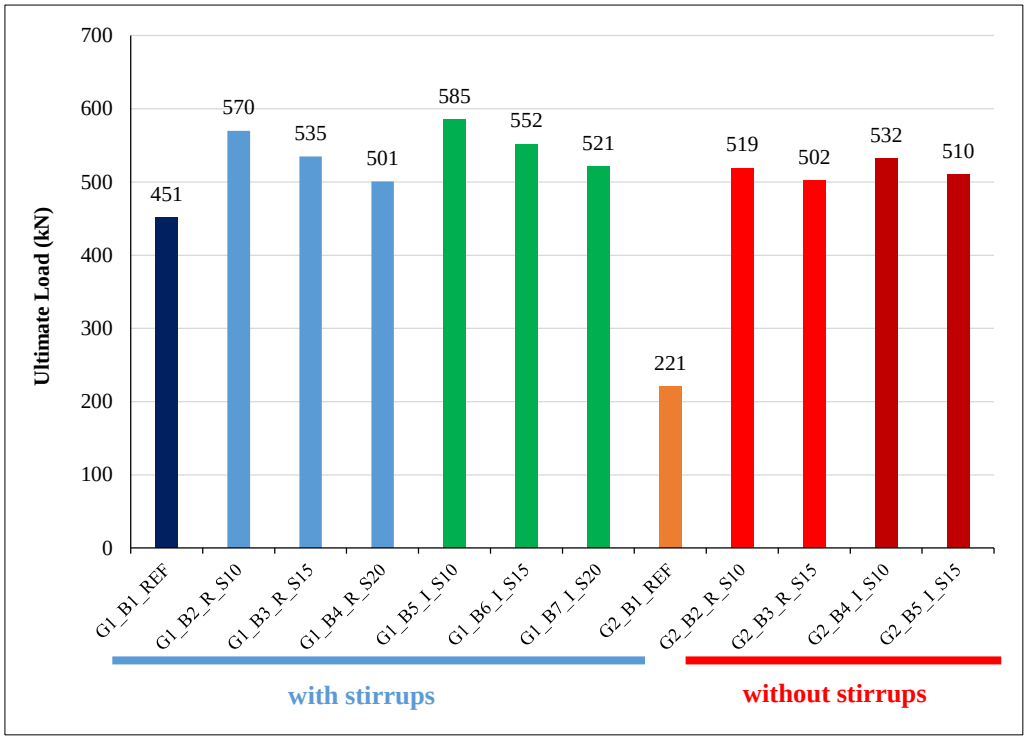

Figure 27. Ultimate load of all beams

4.3.1. Effect of spacing of the CFRP bars on the ultimate load

In Table 12, the ultimate load of the reference beams in Group 1 with vertical CFRP bars increased by 26.4%, 18.6%, and 11.1% for beams with CFRP bar spacings of 10, 15, and 20 cm, respectively. Moreover, the ultimate load of the reference beams in group one with inclined CFRP bars (45°) increased by 29.7%, 22.4%, and 15.5% for beams with CFRP bar spacings of 10, 15, and 20 cm, respectively. This finding indicates that the increasing spacing of the CFRP bars is inversely proportional to beam stiffness for the exact angle of inclination.

According to Table 14, the ultimate load of the reference beams in Group 2 with vertical CFRP bars increased by 135% and 127% for beams with CFRP bar spacings of 10 and 15 cm, respectively. Meanwhile, the ultimate load of the reference beams in group two with inclined CFRP bars (45°) increased by 141% and 131% for beams with CFRP bar spacings of 10 and 15 cm, respectively. This result indicates that the increasing spacing of the CFRP bars is inversely proportional to the ultimate load for the same angle of inclination. The aforementioned result supports the findings of Rashmi et al. [19].

4.3.2. Effect of the angle of inclination of the CFRP bars on the ultimate load

In group one (with stirrups), the beam with inclined CFRP bars (45°) and a spacing of 10 cm has an ultimate load higher than that with vertical CFRP bars (90°) with a similar spacing by 2.6%, as shown in Table 15.

Table 15. Ultimate load of the beams of group one with a CFRP bar spacing of 10 cm

Beam ID	Failure load P_{ult} (kN)	% increase in the ultimate load with respect to Ref.
G1-B2-R-S10	570	Ref.
G1-B5-I-S10	585	2.6

In group two (without stirrups), the beam with inclined CFRP bars (45°) and a spacing of 10 cm has an ultimate load higher than that with vertical CFRP bars (90°) with a similar spacing by 2.5%, as shown in Table 16.

Table 16. Ultimate load of the beams of group two with a CFRP bar spacing of 10 cm

Beam ID	Failure load P_{ult} (kN)	% increase in the ultimate load concerning Ref.
G2-B2-R-S10	519	Ref.
G2-B4-I-S10	532	2.5

In group one (with stirrups), the beam with inclined CFRP bars (45°) and a spacing of 15 cm has an ultimate load higher than that with vertical CFRP bars (90°) with a similar spacing by 3.2%, as shown in Table 17.

Table 17. Ultimate load of the beams of group one with a CFRP bar spacing of 15 cm

Beam ID	Failure load P_{ult} (kN)	% increase in the ultimate load concerning Ref.
G1-B3-R-S15	535	Ref.
G1-B6-I-S15	552	3.2

In group two (without stirrups), the beam with inclined CFRP bars (45°) and a spacing of 15 cm has an ultimate load higher than that with vertical CFRP bars (90°) with a similar spacing of 1.6%, as shown in Table 18.

Table 18. Ultimate load of the beams of group two with a CFRP bar spacing of 15 cm

Beam ID	Failure load P_{ult} (kN)	% increase in the ultimate load concerning Ref.
G2-B3-R-S15	502	Ref.
G2-B5-I-S15	510	1.6

In group one (with stirrups), the beam with inclined CFRP bars (45°) and a spacing of 20 cm has an ultimate load higher than that with vertical CFRP bars (90°) with a similar spacing by 4%, as shown in Table 19.

Table 19. Ultimate load of the beams of group one with a CFRP bar spacing of 20 cm

Beam ID	Failure load P_{ult} (kN)	% increase in the ultimate load concerning Ref.
G1-B4-R-S20	501	Ref.
G1-B7-I-S20	521	4

The beam with inclined CFRP bars (45°) has ultimate load higher than that with vertical CFRP bars (90°) with a similar spacing. This result supports the findings of Van Hong Bui et al. [20].

4.4. Load vs. Strain of the Steel Stirrups

The strain was measured in the second steel stirrups from support (Ø8 mm) by using 5 mm base length electrical strain gauges (FLAB-5-11-3LJC-F) attached to the outer surface of the vertical leg of the stirrup.

Figures 28 and 29 demonstrate that the behaviour of all reinforced beams is practically linear from the beginning of loading up to roughly 60 kN, and the strains created are extremely minor. The un-strengthened control beam in every group displays a greater increase in strain at higher loading stages than the strengthened beams. Moreover, the strain suddenly increased when cracking occurred. Reducing the spacing of the CFRP bars demonstrates better beam stiffness plainly by lowering the produced strains at the same load level. The inclined CFRP bars also demonstrated better beam stiffness than the vertical bars. All the beams in the two groups surpassed the yield strength of the steel bars (2615 με) at ultimate load.

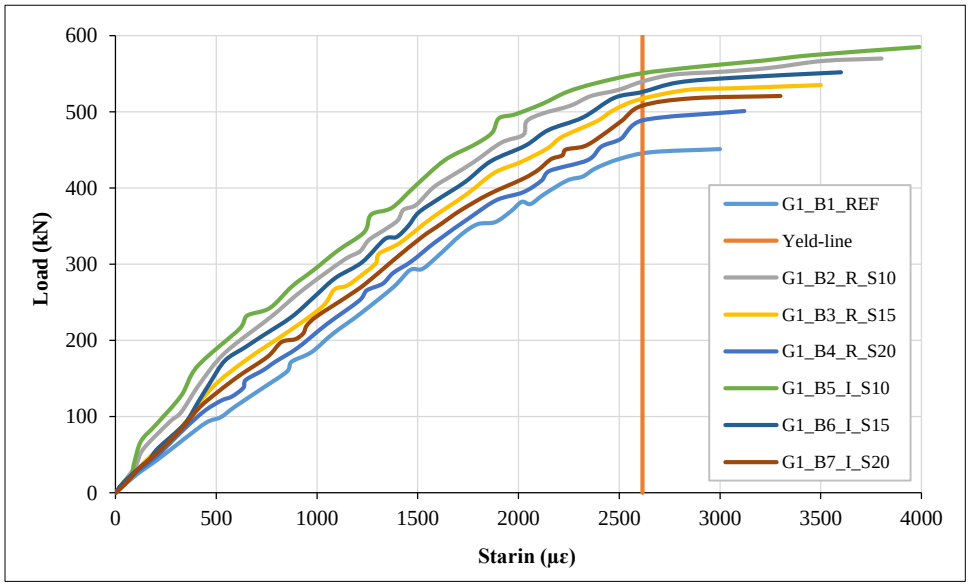

Figure 28. Load versus strain of the steel stirrups of the group one beams

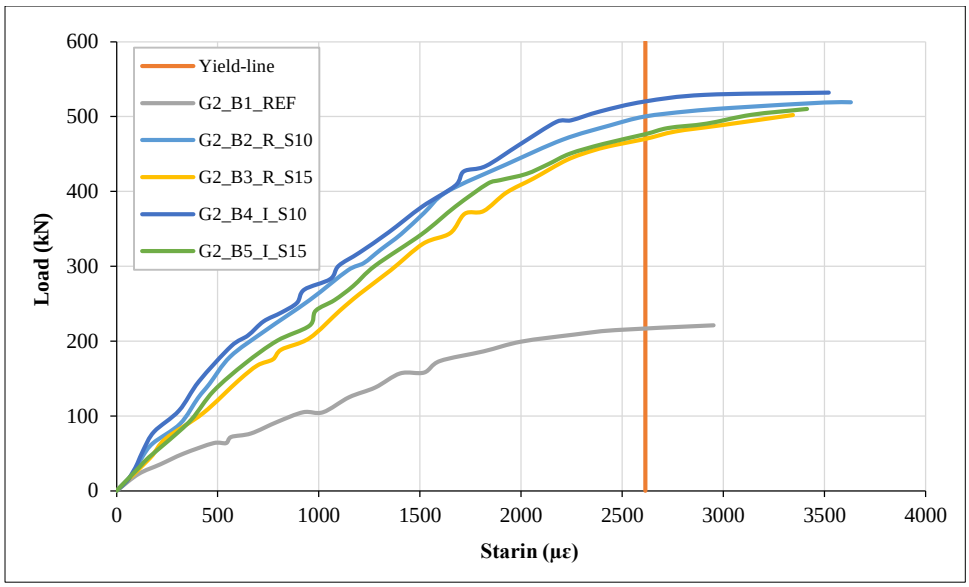

Figure 29. Load versus strain of the steel stirrups of the group two beams

5. Conclusions

- The first crack of the beams of group one occurred at the applied load (60 kN to 80 kN) with a varying first crack load (Pcr)/ultimate load (Pu) percent (11.2% to 14.5%). By contrast, the first crack of the beams of group two occurred at the applied load (50 kN to 80 kN) with a different first crack load (Pcr)/ultimate load (Pu) percent (11.8% to 22.6%).
- The (Pcr/Pu) percent values of all beams were close except those of the beam without CFRP or shear stirrups, which was high. Thus, the effect of the CFRP bars on the Pcr/Pu percent was insignificant.
- At the stage of service load, the mid-span deflection rates of the reference beams of group one (with stirrups) with vertical CFRP bars and a spacing of 20 cm and inclined CFRP bars and a spacing of 10 cm decreased by 0.22% to 14.4%. Meanwhile, the mid-span deflection of the reference beam of group two (without stirrups) increased by 31% to 55% with inclined CFRP bars and a spacing of 10 cm and vertical CFRP bars and a spacing of 15 cm.
- The ultimate load of the reference beams of group one (with stirrups) with vertical CFRP bars and spacings of 10, 15 and 20 cm increased by 26.4%, 18.6% and 11.1%, respectively. Meanwhile, the ultimate load of the reference beams of group one with inclined CFRP bars (45°) and spacings of 10, 15 and 20 cm increased by 29.7%, 22.4% and 15.5%, respectively. This finding indicates that the increasing spacing of the CFRP bars is inversely proportional with the beam stiffness for the exact angle of inclination.
- In group one (with stirrups), the beam with inclined CFRP bars (45°) and a spacing of 10 cm has an ultimate load higher than that with vertical CFRP bars (90°) with a similar spacing by 2.6%. By contrast, the beam with inclined CFRP bars (45°) and a spacing of 10 cm in group two (without stirrups) has an ultimate load higher than that with vertical CFRP bars (90°) with a similar spacing by 2.5%. This finding indicates that the inclined CFRP bars (45°) are approximately better than the vertical ones.
- Reducing the spacing of the CFRP bars by lowering the produced strains at the same load level demonstrates better beam stiffness. Moreover, the inclined CFRP bars exhibited better beam stiffness than the vertical bars. All the beams in the two groups surpassed the yield strength of steel bars (2615 $\mu\varepsilon$) at ultimate load.

6. Declarations

6.1. Author Contributions

Conceptualization, H.H.A. and M.H.A.; methodology, H.H.A. and M.H.A.; investigation, H.H.A.; writing—original draft preparation, H.H.A. and M.H.A.; writing—review and editing, H.H.A. and M.H.A. All authors have read and agreed to the published version of the manuscript.

6.2. Data Availability Statement

The data presented in this study are available upon request from the corresponding author.

6.3. Funding

The authors received no financial support for the research, authorship, and/or publication of this article.

6.4. Conflicts of Interest

The authors declare no conflict of interest.

7. References

[1] Jalil, A., & Al-Zuhairi, A. H. (2022). Behavior of Post-Tensioned Concrete Girders Subject to Partially Strand Damage and Strengthened by NSM-CFRP Composites. Civil Engineering Journal (Iran), 8(7), 1507–1521. doi:10.28991/CEJ-2022-08-07-013.

[2] Abdulkareem, B., & Izzet, A. F. (2022). Serviceability of Post-fire RC Rafters with Openings of Different Sizes and Shapes. Journal of Engineering, 28(1), 19–32. doi:10.31026/j.eng.2022.01.02.

[3] Abbas, H. Q., & Al-Zuhairi, A. H. (2022). Usage of EB-CFRP for Improved Flexural Capacity of Unbonded Post-Tensioned Concrete Members Exposed to Partially Damaged Strands. Civil Engineering Journal (Iran), 8(6), 1288–1303. doi:10.28991/CEJ-2022-08-06-014.

[4] Tuma, N. K., Al-Ahmed, A. H., & Al-Farttoosi, M. H. (2020). The shear strengthening of reinforced concrete beams by embedded through section technique -analytical study-. IOP Conference Series: Materials Science and Engineering, 888(1). doi:10.1088/1757-899X/888/1/012039.

[5] Mhanna, H. H., Hawileh, R. A., & Abdalla, J. A. (2019). Shear strengthening of reinforced concrete beams using CFRP wraps. Procedia Structural Integrity, 17, 214–221. doi:10.1016/j.prostr.2019.08.029.

[6] Abdulkareem, B. F., & Izzet, A. F. (2022). Residual post fire strength of non-prismatic perforated beams. IOP Conference Series: Earth and Environmental Science, 961(1), 012002. doi:10.1088/1755-1315/961/1/012002.

[7] Belarbi, A., Bae, S. W., & Brancaccio, A. (2012). Behavior of full-scale RC T-beams strengthened in shear with externally bonded FRP sheets. Construction and Building Materials, 32(1), 27–40. doi:10.1016/j.conbuildmat.2010.11.102.

[8] Hamid, N. A. A., Thamrin, R., & Ibrahim, A. (2013). Shear Capacity of Non-Metallic (FRP) Reinforced Concrete Beams with Stirrups. International Journal of Engineering and Technology, 5(5), 593–598. doi:10.7763/ijet.2013.v5.624.

[9] Ozden, S., Atalay, H. M., Akpinar, E., Erdogan, H., & Vulaş, Y. Z. (2014). Shear strengthening of reinforced concrete T-beams with fully or partially bonded fibre-reinforced polymer composites. Structural Concrete, 15(2), 229–239. doi:10.1002/suco.201300031.

[10] Said, M., Adam, M. A., Mahmoud, A. A., & Shanour, A. S. (2016). Experimental and analytical shear evaluation of concrete beams reinforced with glass fiber reinforced polymers bars. Construction and Building Materials, 102(1), 574–591. doi:10.1016/j.conbuildmat.2015.10.185.

[11] Issa, M. A., Ovitigala, T., & Ibrahim, M. (2016). Shear Behavior of Basalt Fiber Reinforced Concrete Beams with and without Basalt FRP Stirrups. Journal of Composites for Construction, 20(4). doi:10.1061/(asce)cc.1943-5614.0000638.

[12] Fan, X., Zhou, Z., Tu, W., & Zhang, M. (2021). Shear behaviour of inorganic polymer concrete beams reinforced with basalt FRP bars and stirrups. Composite Structures, 255(1). doi:10.1016/j.compstruct.2020.112901.

[13] Alwash, D., Kalfat, R., Al-Mahaidi, R., & Du, H. (2021). Shear strengthening of RC beams using NSM CFRP bonded using cement-based adhesive. Construction and Building Materials, 301(1), 124365. doi:10.1016/j.conbuildmat.2021.124365.

[14] Bui, L. V. H., Klippathum, C., Prasertsri, T., Jongvivatsakul, P., & Stitmannaithum, B. (2022). Experimental and Analytical Study on Shear Performance of Embedded Through-Section GFRP-Strengthened RC Beams. Journal of Composites for Construction, 26(5), 4022046. doi:10.1061/(asce)cc.1943-5614.0001235.

[15] Peng, K. Di, Huang, J. Q., Huang, B. T., Xu, L. Y., & Dai, J. G. (2023). Shear strengthening of reinforced concrete beams using geopolymer-bonded small-diameter FRP bars. Composite Structures, 305(1), 116513. doi:10.1016/j.compstruct.2022.116513.

[16] ACI 318-19. (1989). Building Code Requirements for Structural Concrete. American Concrete Institute (ACI), Michigan, United States.

[17] ACI 440.2R-17. (2017). Guide for the Design and Construction of Externally Bonded FRP Systems for Strengthening of Concrete Structures. American Concrete Institute (ACI), Michigan, United States.

[18] Mansur, M. A., Huang, L. M., Tan, K. H., & Lee, S. L. (1992). Deflections of reinforced concrete beams with web openings. ACI Structural Journal, 89(4), 391–397. doi:10.14359/3019.

[19] Rashmi, M., Anand, V. N., & Balaji, N. C. (2021). Shear strengthening of RC beams using near surface mounted technique with glass fiber reinforced polymer. AIP Conference Proceedings. doi:10.1063/5.0039664.

[20] Van Hong Bui, L., Stitmannaithum, B., & Ueda, T. (2020). Experimental Investigation of Concrete Beams Strengthened with Embedded Through-Section Steel and FRP Bars. Journal of Composites for Construction, 24(5), 4020052. doi:10.1061/(asce)cc.1943-5614.0001055.